Available online at www.sciencedirect.com
ScienceDirect
Catalysis Today 125 (2007) 64–73
CATALYSIS TODAY
www.elsevier.com/locate/cattod

Comparison of performance of microreactor and semi-batch reactor for catalytic hydrogenation of *o*-nitroanisole

Sunitha Tadepalli *, Dongying Qian, Adeniyi Lawal

New Jersey Center for Microchemical Systems, Department of Chemical, Biomedical and Materials Engineering, Stevens Institute of Technology, Hoboken, NJ 07030, United States

Available online 5 April 2007

Abstract

Hydrogenation reactions are ubiquitous in the fine chemicals and pharmaceutical industries. Conventionally, the kinetic studies of hydrogenation reactions are conducted in slurry or batch reactors. The kinetics of fast hydrogenation reactions is often difficult to study in a batch reactor because of the poor mass transfer characteristics of this system. The use of a microchannel reactor for such reactions provides improved mass transfer rates which may ensure that the reaction operates close to intrinsic kinetics. In the present study, a laboratory semi-batch reactor (25 mL) and a packed-bed microreactor (775 μm ID) were evaluated to determine the reactor system that would be best suited for conducting the kinetic study of hydrogenation reactions. For this purpose, hydrogenation of *o*-nitroanisole to *o*-anisidine in methanol was selected as a model three-phase reaction. The reaction rates in the two reactor systems were found to be similar under the conditions used for kinetic experiments. Therefore, both batch and microreactors are suitable for studying the kinetics of this reaction. Subsequently, the two reactors were modeled and the modeling results were used to determine the mass transfer coefficients in the two systems under typical operating conditions. The mass transfer coefficients in the microreactor were found to be two orders of magnitude higher than in the semi-batch reactor. This order of magnitude difference in the mass transfer coefficients enables the microreactor to obtain intrinsic kinetics data for fast hydrogenation reactions with half lives in the order of magnitude between 10^0 and 10^2 s.

Keywords: Catalytic hydrogenation; Fixed-bed microreactor; Semi-batch reactor; Reactor modeling; Kinetics; Mass transfer analysis

1. Introduction

Catalytic hydrogenation has evolved as a key process for the manufacture of fine chemicals and pharmaceuticals constituting about 10–20% of all the reactions in the pharmaceutical industry [1]. For example, catalytic hydrogenation of nitro compounds is important in the synthesis of drugs such as Viagra, Zyvox, Agenerase [2] and antimalarial drugs [3]. Similarly, hydrogenation of 2,4-dinitro toluene to toluene diamine is an important step in the production of polyurethane [3] and in the manufacture of TDI (toluene di-isocyanate), a fine chemical [4]. The diverse applications of catalytic hydrogenation lead to significant advances in the way these reactions are conducted in the pharmaceutical and fine chemical industries.

Various types of reactor designs such as trickle bed [5], fixed bed [6] and slurry [4,7] reactors have been used in commercial operation. The types of reactor systems used for multi-phase hydrogenation reactions depend upon the type of reaction and the phase behavior of the catalyst and the reactants. All three-phase processes involve steps of gas–liquid, liquid–solid and intra-particle mass transfer and chemical reaction. The relative importance of these individual steps depends upon the type of contact between these phases provided by the reactor system. Therefore, the choice of the reactor is important for optimum performance.

In the pharmaceutical industry, most of the multi-phase hydrogenation reactions are conducted in large slurry batch or semi-batch reactors, where the catalyst is suspended in the liquid, which is continuously agitated with a stirrer. The interest in slurry batch reactors derives from their industrial importance in the manufacture of important intermediates for dyes, agrochemicals and pharmaceuticals, often produced on a large industrial scale [3]. Also, the laboratory semi-batch reactor or

* Corresponding author. Tel.: +1 201 216 5332.
E-mail address: stadepal@stevens.edu (S. Tadepalli).

0920-5861/$ – see front matter
doi:10.1016/j.cattod.2007.01.076

Nomenclature

a	mass of the catalyst per unit volume of the microreactor (g/L)
a_1	mass of the catalyst per unit volume of the semi-batch reactor (g/L)
$C_{anisidine}$	concentration of anisidine (mol/L)
C_A	concentration of limiting reactant (mol/L)
$C_{hydrogen}$	concentration of hydrogen (mol/L)
$C_{H,b}$	concentration of the hydrogen in the bulk liquid (mol/L)
$C_{H,c}$	concentration of the hydrogen at the catalyst surface (mol/L)
$C_{H,sat}$	saturation concentration of hydrogen at the gas–liquid interface obtained from the hydrogen solubility data (mol/L)
C_{H_2}	concentration of hydrogen (mol/L)
$C_{intermediate}$	concentration of intermediate (mol/L)
C_{nitro}	concentration of nitroanisole (mol/L)
C_N	concentration of nitroanisole (mol/L)
$k_{gl}a_{gl}$	liquid side mass transfer coefficient (s^{-1})
$k_{ls}a_{ls}$	liquid/solid mass transfer coefficient (s^{-1})
k_r	intrinsic rate constant (s^{-1})
k_I	intrinsic kinetic rate constant for reaction I (L^2/g h mol)
k_{II}	intrinsic kinetic rate constant for reaction II (mol/g h)
K_N	equilibrium constant for nitroanisole in reaction I (L/mol)
K_{H_2I}	equilibrium constant for hydrogen in reaction I (L/mol)
K_{H_2II}	equilibrium constant for hydrogen in reaction II (L/mol)
K_{la}	overall mass transfer coefficient (s^{-1})
K_I	equilibrium constant for intermediate in reaction I (L/mol)
r	reaction rate (mol/L s)
r_1	reaction rate for reaction I (mol/g h)
r_2	reaction rate for reaction II (mol/g h)
t	reaction time (min)
v_l	liquid superficial velocity (cm/s)
z	distance from the entrance of the reactor (cm)

slurry reactor is often used as a tool to provide intrinsic kinetic data, which is used for the design of the large-scale catalytic reactors, and for better understanding of catalytic reaction mechanisms. Several examples of catalytic hydrogenation kinetic studies in batch reactors have been published previously from catalysis and reaction engineering viewpoint [7–9]. However, the kinetic studies for fast hydrogenation reactions are difficult to conduct in a batch reactor even at the highest stirrer speed. This is because for fast hydrogenation reactions the mass transfer effects become predominant over intrinsic kinetics. As a result the true intrinsic kinetic rates of fast hydrogenations reactions are masked by mass transfer limitations in batch reactors leading to reaction times longer than needed for the reaction to be controlled by intrinsic kinetics. For slow hydrogenation reactions, the batch reactor can be used to obtain intrinsic kinetic data. However, the volume of the batch reactor is another variable to determine if the reactor can be used to study intrinsic kinetics. As the volume of the batch reactor increases, there will be problems associated with non-uniform mixing. Inefficient mixing in large batch reactors may shift the process from kinetic region to a mass transfer controlled region [10]. This shift will have significant effect on the conversion, and the selectivity of the desired products.

In recent years, there has been a growing interest in utilizing microreactors for catalytic hydrogenation because of their numerous advantages over conventional reactors. Microchannel reactors with their small transverse dimensions possess extremely high surface to volume ratios and consequently exhibit enhanced heat and mass transfer rates. The small volume of the microreactor enables fast transport of the fluid layers thus reducing the reaction time and providing greater selectivity and higher product yield. The diffusion of gases into the liquid reactant often poses problems of mass transfer in conventional reactors. This can be overcome in microreactors by increasing the interfacial contact area between the two mixing fluids, or by reducing the characteristic length scale thereby forcing a reactant in one phase to mix, diffuse and react with the reactant in the second phase at the catalyst surface, thus improving the rate of mass transfer tremendously.

Several researchers have investigated gas–liquid–solid hydrogenation in microreactors by incorporating the catalyst into microreactors in different forms [11–13]. For example, Kreutzer et al. [11] used monolith reactors for hydrogenation of a nitro aromatic compound and observed several advantages of conducting this fast reaction in the monolith reactor, such as good mass transfer characteristics and low pressure drop. Similarly, Losey et al. [12] used microfabricated packed-bed reactors for the hydrogenation of cyclohexene. They observed that the mass transfer coefficients in the microreactor range from 5 to 15 s^{-1} which are nearly two orders of magnitude larger than the values obtained from laboratory trickle-bed reactors. Gavriilidis et al. [13] also conducted experimental studies on nitrobenzene hydrogenation in a microstructured falling film reactor and observed that the overall mass transfer rate in the microreactor is enhanced significantly with an enormous increase in surface area per unit reaction volume. The excellent mass transfer characteristics of the microreactor enable it to be used as a tool to obtain intrinsic kinetics information for fast hydrogenation reactions. There is limited literature available on the study of intrinsic kinetics of fast hydrogenation reactions in the microreactor in spite of its excellent mass transfer characteristics. Instead, all the kinetic studies were conducted in conventional batch or other reactors which exhibit poor mass transfer and mixing characteristics. These observations have led to the present study where the microreactor and semi-batch reactor were evaluated to study the extent to which these reactors can be used as efficient reactor systems for obtaining intrinsic kinetics data. For this

purpose, hydrogenation of *o*-nitroanisole was chosen as the model gas–liquid–solid reaction.

In our previous contribution, the kinetics of hydrogenation of *o*-nitroanisole reaction were studied in great detail in a packed-bed microreactor and optimum reaction conditions were determined for the final design of a multi-channel reactor [14]. There is limited literature available on the kinetics of this reaction in the slurry batch reactors [7], where the investigators report reaction orders for *o*-nitroanisole and hydrogen between zero and one without describing the role of the intermediate species, which has a significant effect on the reaction rate. The present work includes the study of the kinetics of this reaction in a laboratory semi-batch reactor. The reaction rates in the semi-batch reactor were compared to those of the microreactor to determine the suitability of the two systems for kinetic study for this reaction. Using the kinetic information from the two reactors, the mass transfer coefficients of the two systems were evaluated. These mass transfer coefficients were then used to determine the reactions for which the batch or microreactor would be suitable for conducting kinetic studies.

2. Experimental

In this section a list of the chemicals used for the experiments, and the description of the experimental setup of the semi-batch reactor are provided. The description of the microreactor experimental system was provided in the previous work [14]. The catalyst used was a commercial 2% (w/w) Pd supported on zeolite (aluminum sodium silicate) supplied by FMC. This catalyst was ground and sieved to obtain a particle size in the range of 75–150 μm. The dispersion of palladium on the support was measured using TEM (FEG-TEM, Model CM20, Philips, Eindhoven, The Netherlands) and was calculated to be 36%. The surface area and pore size of the catalyst were 170–220 m^2/g and 10–12 nm, respectively, measured by BET (multi-point BET technique, using Quantochrome Instruments Autosorb-1). The reactant *o*-nitroanisole (99% purity level) and solvent methanol (HPLC grade) were obtained from Sigma–Aldrich. The hydrogen was purchased from Praxair. The mobile phase used for the HPLC analysis comprised de-ionized water and acetonitrile (HPLC grade), the latter was purchased from Pharmco Products Inc.

2.1. Description of the semi-batch reactor

Experiments were conducted in a 25 mL PARR semi-batch slurry reactor (PARR 5500 Series Compact Reactor). Fig. 1 is a schematic of the experimental reactor used for conducting the reaction. The compressed H_2 gas passed through the inlet pressure regulating valve into the reactor which was filled with the liquid reactant and the catalyst. The reactor was equipped with compact magnetic impeller designed to stir at speeds up to 1000 rpm. Heating was provided electrically using a heating coil. A continuous stream of cooling water was circulated around the reactor to control the temperature of the reactor. A thermocouple (T1) was incorporated into the reactor to read the reaction temperature at any given time. The pressure in the reactor was controlled using an electronic pressure controller attached to the gas cylinder. The gas consumption during the experiments was measured from the pressure transducer (P1) attached to the cylinder. The reactor pressure (P2) was maintained at a constant value throughout the experimental run. The reactor was equipped with a pressure relief valve to relieve the pressure at the end of the experiment, and a sampling valve to collect the liquid sample at regular intervals of time.

Before starting any experimental run, the reactor was filled with the liquid reactant and the catalyst, after which it was connected to the experimental system. Then, the reactor was purged with hydrogen to replace any air remaining in the reactor. After the reactor temperature and pressure reached the desired values, the agitator was started and this time was recorded as the starting time of the reaction. The starting time is accurate with an error of less than 10 s. Even this error is attributed to the time for the stirrer to reach the desired stirrer speed. The product was collected from the sampling port at regular intervals of time. These samples were diluted with methanol (HPLC grade) and were analyzed using the high performance liquid chromatography (HPLC) from Shimadzu. A Diode Array detector is used for scanning so that the samples could be scanned at multiple wavelengths at the same time. A method was established in the

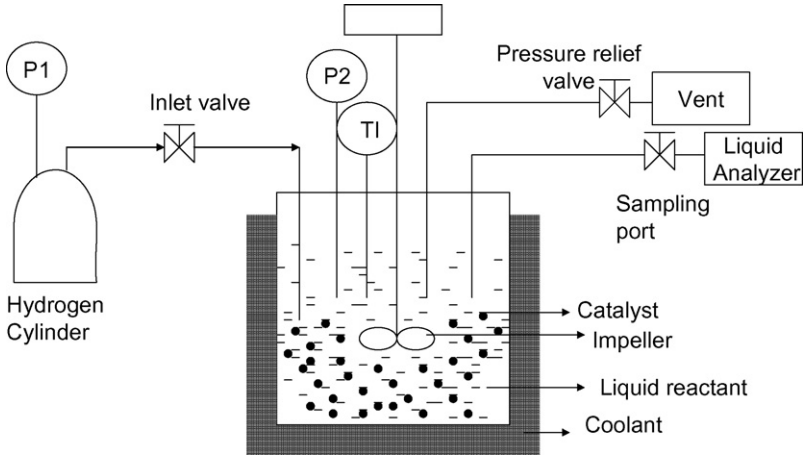

Fig. 1. Batch reactor experimental setup.

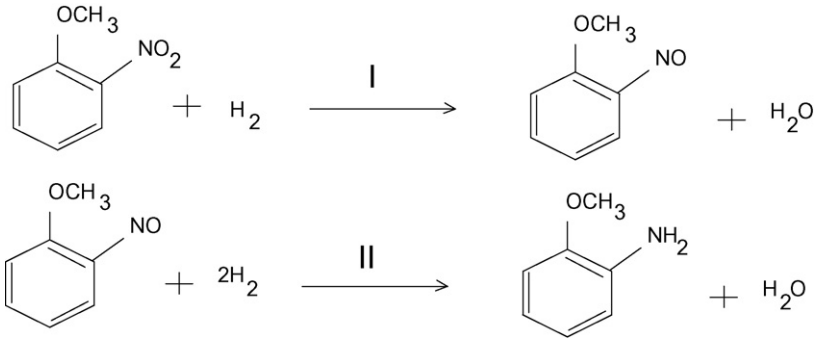

Fig. 2. Reaction pathway for the hydrogenation of *o*-nitroanisole.

HPLC using water and acetonitrile as the mobile phase, in conjunction with an RP C^{18} column from Waters Corporation. Calibration was done for both the reactant and the product using standard solutions. The concentrations of the unknown product samples are determined using the calibration.

3. Results and discussion

3.1. Reaction pathway

The catalytic hydrogenation of *o*-nitroanisole to *o*-anisidine involves a three-step reduction series reaction. First, the reduction of *o*-nitroanisole to 2-methoxynitrosobenzene, next to *N*-(2-methoxyphenyl) hydroxylamine, and, finally to *o*-anisidine. During the experiments only one intermediate was observed in the product stream along with the product, and reactant at all operating conditions. This intermediate was found to be 2-methoxynitrosobenzene by the mass spectrum analysis. The presence of hydroxylamine derivative was not detected during analysis, indicating that it had only transient lifetime probably because of its instantaneous reaction with hydrogen to form *o*-anisidine, the rate of which far exceeds its formation from 2-methoxynitrosobenzene. Thus, the hydrogenation of *o*-nitroanisole to *o*-anisidine was considered as a process consisting of two consecutive reactions, one leading to the formation of 2-methoxynitrosobenzene, and the other leading to the formation of *o*-anisidine as shown in Fig. 2.

3.2. Kinetic study in the semi-batch reactor

In order to study the kinetics of this reaction, first the effect of external mass transfer was studied as a function of agitation speed to obtain the stirrer speed beyond which the reaction rate did not change with speed. Then, the intrinsic kinetics of the reaction was investigated by studying the effect of reactants concentration on the initial rate of the reaction. Pore diffusion or internal mass transfer effect is assumed negligible based on the results obtained in the microreactor using particle sizes in the range 45–75 and 75–150 μm [14].

3.2.1. Effect of stirrer speed on rate of reaction and selectivity of anisidine

Experiments were done at different stirrer speeds to determine the speed at which the external mass transfer effect can be considered to be negligible. Fig. 3 shows the effect of stirrer speed on average reaction rate and *selectivity* of anisidine. *Selectivity* is defined as the ratio of the number of moles of the desired product formed to the moles of the product that would have been formed if there were no side reactions. At low stirrer speeds, both the rate and selectivity increase with increase in stirrer speed. However, when the stirrer speed is increased beyond 600 rpm, it has no further effect on the rate and also on the selectivity. At low stirrer speeds the mass transfer effect may have some influence on the rate, while above 600 rpm stirrer speed the reaction is controlled by the intrinsic kinetics. The low selectivity values at low stirrer speeds was due to the presence of the intermediate, 2-nitrosomethoxybenzene. At high stirrer speeds the intermediate might be reacting faster, resulting in high anisidine selectivity.

3.2.2. Initial rate analysis

Experiments were conducted at 800 rpm under different nitroanisole and hydrogen concentrations to determine the intrinsic kinetic rate expression for the reaction in a semi-batch reactor. The catalyst loading was kept small (<7 mg) for all the kinetic experiments. For reproducibility purpose, all the experiments have been repeated at least twice. Fig. 4 shows that there is a wide range of linear relationship of concentration

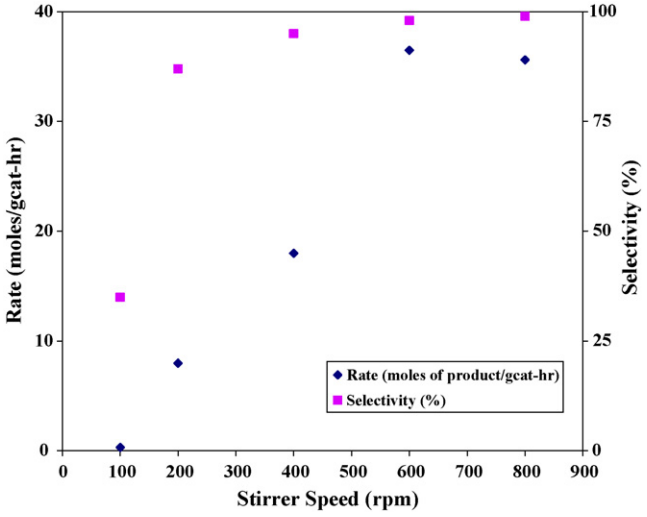

Fig. 3. Effect of stirrer speed on the reactor performance (20 mg of 2% Pd/zeolite catalyst, 30 °C reactor temperature, initial nitroanisole concentration = 1.299 mol/L and reactor pressure = 100 psig).

of reactant and product versus time close to time $t = 0$. For the kinetic study, the initial rates of hydrogenation were calculated from the slope of these lines. The dependence of initial rate of disappearance of nitroanisole and initial rate of formation of anisidine on hydrogen and nitroanisole concentrations is determined as follows.

Dependence of rate of disappearance of nitroanisole on hydrogen concentration. The effect of hydrogen concentration on the rate of disappearance of nitroanisole was studied by varying the hydrogen pressure, keeping the values of the other variables including nitroanisole concentration constant. The concentration of hydrogen in the liquid at different pressures was obtained from the solubility data for H_2 in a mixture of *o*-nitroanisole–methanol from the work of Brahme et al. [15]. Fig. 5 shows the effect of hydrogen concentration on the rate of disappearance of nitroanisole obtained at three temperature levels of 30, 40 and 50 °C, at a nitroanisole concentration of 1.29 mol/L. The data show that the reaction rate increases with hydrogen concentration in the liquid. The error bars in these plots were calculated by replicating the runs at least twice. They represent the error in obtaining the initial rate data or in other words the error in being able to extrapolate the curve towards zero.

Dependence of rate of disappearance of nitroanisole on nitroanisole concentration. Fig. 6 shows the rate of disappearance of nitroanisole with nitroanisole concentration keeping all variables including hydrogen pressure (100 psig) or concentration constant. The rate of disappearance of nitroanisole increases with increase in nitroanisole concentration up to a certain concentration, and then remains constant for all temperatures.

Dependence of rate of formation of o-anisidine on hydrogen concentration. Fig. 7 shows the effect of hydrogen concentration on the rate of formation of anisidine obtained at three temperature levels of 30, 40 and 50 °C, keeping the values of the other variables, including nitroanisole concentration, constant. The rate increases with increase in hydrogen concentration.

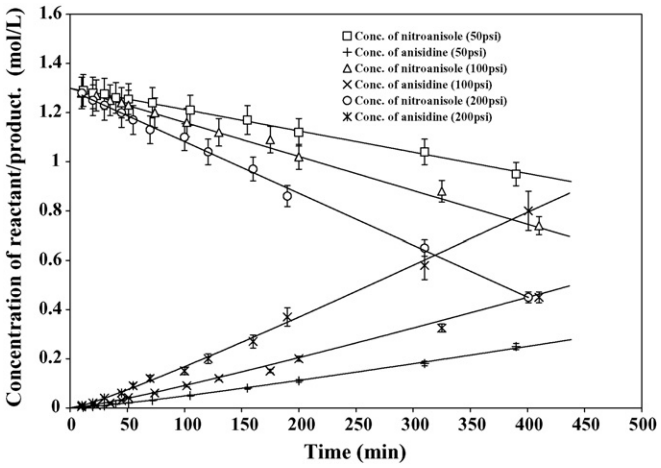

Fig. 4. Concentration of nitroanisole and anisidine vs. time at different hydrogen pressures.

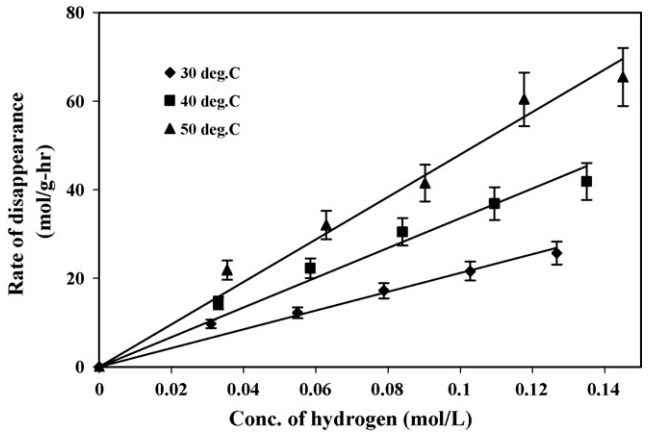

Fig. 5. Rate of disappearance of nitroanisole with hydrogen concentration.

Dependence of rate of formation of o-anisidine on nitroanisole concentration. Fig. 8 shows the rate of formation of anisidine at different nitroanisole concentrations in a semi-batch reactor at constant hydrogen pressure. The rate first increases with *o*-nitroanisole concentration, attains a maximum value and then decreases with further increase in *o*-nitroanisole concentration. The decrease in the rate of *o*-anisidine formation at high concentrations of *o*-nitroanisole is due to substrate

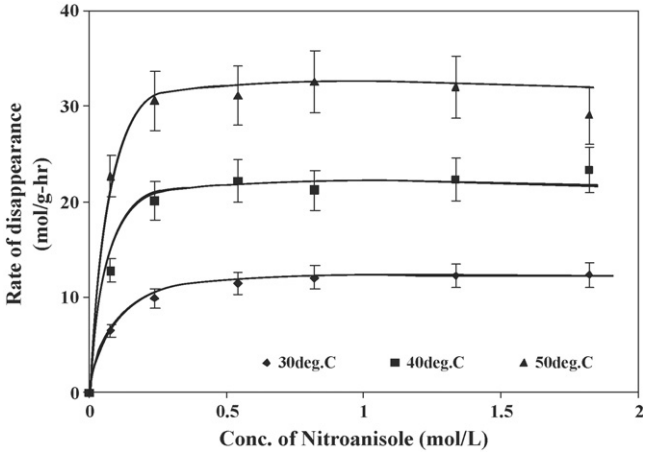

Fig. 6. Rate of disappearance of *o*-nitroanisole with *o*-nitroanisole concentration.

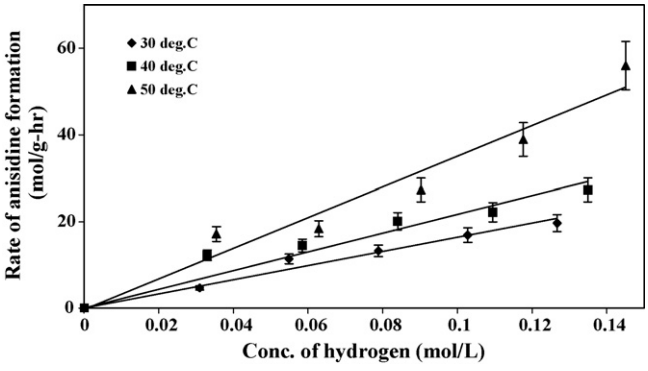

Fig. 7. Rate of formation of anisidine with hydrogen concentration.

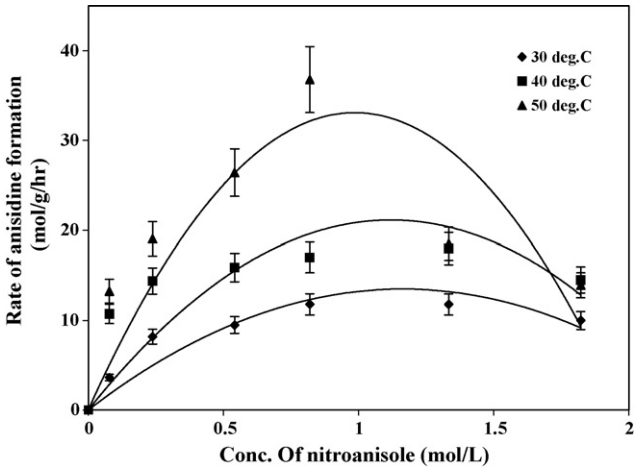

Fig. 8. Rate of formation of anisidine at different nitroanisole concentrations.

inhibition effect present at high concentrations. A comparison of the data of Figs. 6 and 8 shows that the rate of disappearance of nitroanisole is somewhat higher than the rate of formation of anisidine at same conditions especially at high nitroanisole concentrations. This indicates that the intermediate 2-methoxy nitrosobenzene is present in the product stream as a by-product, which was also observed while conducting kinetic experiments in the microreactor [14].

3.2.3. Kinetic modeling

The initial rate data obtained were fitted to different rate equations based on Langmuir–Hinshelwood (L–H) or Eley-Rideal type models. A non-linear regression analysis (Levenberg–Marquardt (LM) algorithm using Polymath 5.1) was performed in order to estimate the kinetic constants for the individual rate equations. For regression analysis, the rate expressions that best fitted the microreactor data [14] (Eqs. (1) and (2) for reactions I and II, respectively) were first used to fit the semi-batch experimental data. These equations were also found to be the best fit for semi-batch data.

- For reaction I (desorption of the product controlling):

$$r_1 = \frac{k_I C_{H_2} C_N}{(1 + K_N C_N)(1 + K_{H_2I} C_{H_2})} \quad (1)$$

- For reaction II (surface reaction controlling):

$$r_2 = \frac{k_{II} K_{H_2II} C_{H_2} K_I C_I}{(1 + K_I C_I)(1 + K_{H_2II} C_{H_2})} \quad (2)$$

where k_I and k_{II} are the rate constants for reactions I and II, respectively, K_N, K_{H_2I}, K_I and K_{H_2II} are adsorption equilibrium constants, C_{H_2}, C_N and C_I are concentrations of hydrogen, *o*-nitroanisole and 2-nitrosomethoxybenzene, respectively. The concentration of intermediate (C_I) was calculated from material balance.

The values of the kinetic constants for these models are given in Table 1. The rates predicted from the rate equations agree with the experimental rates within 10%. The activation energies for reactions I and II were determined from the kinetic constants using Arrhenius equations. The values are 46.3 and 11.9 kJ/mol for reactions I and II, respectively, which compare favorably to the literature value of 43.83 kJ/mol [7] for reaction I.

Table 1
Kinetic constants and regression coefficients for the reactions in semi-batch reactor

Temperature (°C)	k_I (L^2/g h mol)	K_N (L/mol)	K_{H_2I} (L/mol)	R^2
Reaction I				
30	2087.31 ± 35.12	6.05 ± 0.12	5.65 ± 0.29	0.957
40	3766.19 ± 4.25	7.06 ± 0.01	4.01 ± 0.017	0.987
50	6518.78 ± 8.29	11.11 ± 0.01	1.29 ± 0.013	0.988
Temperature (°C)	k_{II} (mol/g h)	K_I (L/mol)	K_{H_2II} (L/mol)	R^2
Reaction II				
30	151.53 ± 0.42	98.97 ± 1.11	1.58 ± 0.01	0.94
40	172.52 ± 0.15	61.59 ± 0.28	1.81 ± 0.01	0.94
50	202.99 ± 2.10	9.86 ± 0.17	7.33 ± 0.13	0.936

In order to further establish the validity of the above rate equations, and associated kinetic parameters of the overall reaction, a comparison was made between the experimental data obtained under integral conditions, and the theoretical predictions from the above rate equations. To derive the integral model based on the rate equations, the following assumptions were made: (1) there are no mass transfer limitations, and (2) change in the volume due to the reaction is negligible.

The rate of change of concentrations of *o*-nitroanisole, intermediate, hydrogen and *o*-anisidine per unit time are given by the following equations:

$$\frac{dC_{nitro}}{dt} = a_1(-r_1) \quad (3)$$

$$\frac{dC_{intermeiate}}{dt} = a_1(r_1 - r_2) \quad (4)$$

$$\frac{dC_{hydrogen}}{dt} = a_1(-r_1 - 2r_2) \quad (5)$$

$$\frac{dC_{anisidine}}{dt} = a_1(r_2) \quad (6)$$

where C_{nitro}, $C_{intermediate}$, $C_{hydrogen}$ and $C_{anisidine}$ are the concentrations of *o*-nitroanisole, intermediate, hydrogen and *o*-anisidine, respectively, at the given instance, a_1 is the density of catalyst per unit volume of the reactor, and r_1 and r_2 are the reaction rates from Eqs. (1) and (2), respectively. Eqs. (3)–(6) were solved using Runge–Kutta method with the following initial conditions: at $t = 0$, $C_{nitro} = 1.299$ mol/L, $C_{intermediate} = 0$ and $C_{anisidine} = 0$, temperature = 30 °C, pressure = 100 psig and catalyst loading = 20 mg. The model predictions and experimental data for the conversion of *o*-nitroanisole under these operating conditions are shown in Fig. 9, and are within 5–10% of each other. This excellent agreement suggests that the rate parameters determined here represent the results obtained under integral conditions.

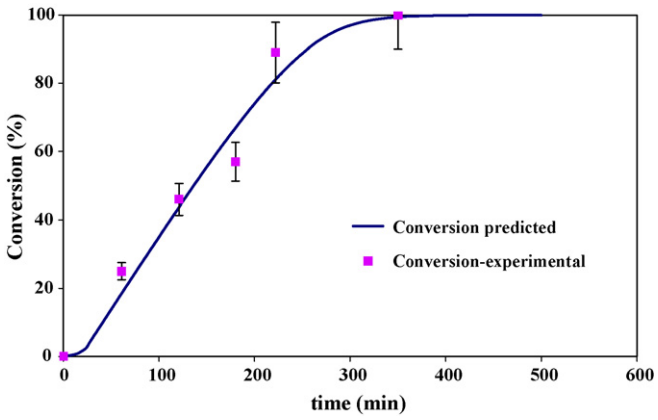

Fig. 9. Experimental and predicted conversion of *o*-nitroanisole for a semi-batch reactor.

3.3. Comparison of performance of microreactor with the semi-batch reactor

3.3.1. Comparison of reaction rates

A comparison between the microreactor and the semi-batch reactor was made based on the intrinsic rates obtained in two systems for this reaction. Fig. 10 shows the comparison of initial reaction rate for the semi-batch reactor and the reaction rate obtained for a differential microreactor (results presented in [14]) under similar reaction conditions. The data in Fig. 10 shows that the reaction rates of both reactors are the same under similar conditions. This confirms that the kinetic data obtained in both reactors are free of any external mass transfer effects, thus indicating that the microreactor is as efficient as the semi-batch reactor in obtaining intrinsic kinetic data for this reaction. Therefore, this reaction can be considered as a slow hydrogenation reaction where the mass transfer limitations in the batch reactor are negligible and the reaction can be assured to be controlled by intrinsic kinetics. However, it should be noted that the batch reactor used for these experiments has a volume of 25 mL. As the volume of the batch reactor increases, there is a substantial decrease in mass transfer efficiency due to inefficient mixing in large volume of the batch reactor. Hence, it is likely that the reaction may shift from kinetic region to mass transfer region with increase in reactor volume. Therefore, it is important to evaluate the mass transfer efficiency of the reactor system before conducting experiments to study the intrinsic kinetics of the reaction.

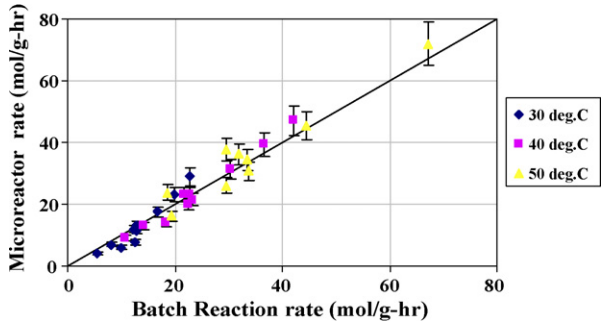

Fig. 10. Comparison of reaction rates of microreactor and batch reactor.

3.3.2. Mass transfer analysis

Using the intrinsic kinetic information and the mass transfer equations, the semi-batch reactor and microreactor were modeled. The modeling results were used to evaluate the mass transfer parameters. Unlike the modeling done in Section 3.2.3, where mass transfer effects were neglected, the modeling in this section includes different mass transfer steps of hydrogen, starting with diffusion of hydrogen from the gas phase to the liquid and from the liquid to the catalyst surface. The modeling calculations were performed using Athena Visual Workbench package (v.8.3, Stewart & Associates Engineering Software, Inc.) and these results were compared to the experimental data for an integral reactor to estimate the overall mass transfer coefficient for the two reactor systems under different reaction conditions.

3.3.2.1. Modeling of microreactor. The microreactor model was based on the Taylor flow regime. This is a typical two-phase flow pattern in the microchannel [16] which consists of alternate gas and liquid slugs separated by a well defined boundary. This type of flow is most commonly found in small diameter tubes [17]. We conducted flow visualization experiments in a glass microreactor with a square cross-section measuring 500 μm × 500 μm packed with glass beads of the same size range as the catalyst particles used in all experiments. These experiments showed that Taylor flow regime exists in a packed-bed microreactor, except that slug boundaries are broken-up by the particles. With this type of flow, hydrogen from the gas phase is being depleted in two ways. From the gas slug, hydrogen is transferred to the thin film surrounding the catalyst, and also to the liquid slug through the gas–liquid interface. The schematic representation of these mass transfer steps are depicted in Fig. 11. For modeling of the microreactor, the intrinsic rate expressions were obtained from our earlier studies [14] where we investigated the kinetics of the reaction in great detail in the microreactor. The mass transfer equations used for modeling the microreactor are based on Nijhuis et al. [17] model for a monolith reactor. These equations are given below.

3.3.2.2. Model for microreactor.

- Hydrogen concentration in bulk liquid

$$v_l \frac{dC_{H,b}}{dz} = k_{ls}a_{ls}(C_{H,c} - C_{H,b}) + k_{gl}a_{gl}(C_{H,sat} - C_{H,b}) \quad (7)$$

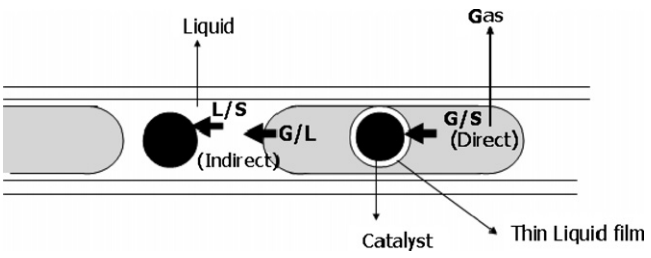

Fig. 11. Schematic representation of mass transfer steps in a packed-bed microreactor.

• Hydrogen at catalyst

$$k_{ls}a_{ls}(C_{H,b} - C_{H,c}) = a(r_1 - r_2) \quad (8)$$

• *o*-Nitroanisole at the catalyst surface

$$v_l \frac{dC_{nitro}}{dz} = a(-r_1) \quad (9)$$

$$r_1 = \frac{k_1 C_{H,c} C_N}{(1 + K_N C_N)(1 + K_{H_2 1} C_{H,c})} \quad (10)$$

$$r_2 = \frac{k_{II} K_{H_2 II} C_{H,c} K_I C_I}{(1 + K_I C_I)(1 + K_{H_2 II} C_{H,c})} \quad (11)$$

The values of the kinetic constants for Eqs. (10) and (11) are given in Table 2. From Tables 1 and 2, it can be observed that the kinetic constants for the reactions in the two reactor systems are different. However, the reaction rates calculated from these kinetic constants are almost the same under similar conditions. Since the regression analysis does not take into account the experimental error (or error bars), it generates different kinetic constants for slight changes in the experimental data. Therefore, the difference in the kinetic constants for the reactions in the two reactor systems was attributed to regression analysis.

Eqs. (7)–(11) were further simplified by making the following assumptions:

(1) The reaction is taking place in both the gas and liquid slugs and there is no reaction rate oscillation between gas and liquid slugs. This implies that the rate of transport of hydrogen to the catalyst surface is the same in both liquid and gas slugs.
(2) The change in the mass transfer coefficient along the reactor length is negligible.
(3) Since gas–liquid reactions are usually controlled by gas to liquid mass transfer rate, the value of the liquid to solid mass transfer coefficient was assumed to be very high (this was confirmed by calculating the $k_{ls}a_{ls}$ value using correlations in [17,18]).

Using these assumptions, the microreactor was modeled under different reaction conditions. Fig. 12 shows the typical modeling results obtained by solving these differential equations. The figure shows that the concentration of hydrogen in the bulk liquid as well as at the catalyst surface is close to the saturation concentration of hydrogen indicating that external mass transfer resistances are negligible and the reaction is controlled by intrinsic kinetics.

Table 2
Kinetic constants and regression coefficients for the reactions in the microreactor

Temperature (°C)	k_I (L^2/g h mol)	K_N (L/mol)	K_{H_2I} (L/mol)	R^2
Reaction I				
30	620.15 ± 4.06	2.00 ± 0.018	0.24 ± 0.006	0.97
40	1556.07 ± 6.67	3.14 ± 0.017	1.38 ± 0.04	0.984
50	3100.00 ± 18.69	3.93 ± 0.03	2.61 ± 0.06	0.965
Temperature (°C)	k_{II} (mol/g h)	K_I (L/mol)	K_{H_2II} (L/mol)	R^2
Reaction II				
30	149.1 ± 0.045	11.09 ± 0.084	2.25 ± 0.01	0.954
40	216.9 ± 1.57	6.78 ± 0.096	4.02 ± 0.04	0.972
50	404.99 ± 3.75	3.29 ± 0.044	4.41 ± 0.06	0.957

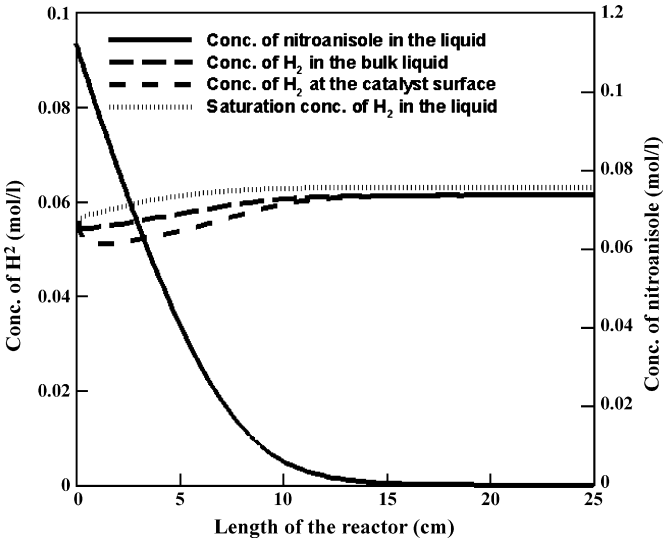

Fig. 12. Modeling results for a packed-bed microreactor at 100 psig pressure, 30 °C temperature, 0.05 mL/min liquid flowrate and 5 sccm gas flowrate, 1.299 mol/L nitroanisole concentration and $k_{gl}a_{gl} = 8\ s^{-1}$.

Experiments were carried out in the microreactor under different operating conditions. The reaction results from these experiments were compared with the theoretical predictions from Eqs. (10) and (11) for an integral reactor with no mass transfer effects. Most of the experimental results agree with these predictions as shown in [14]. However, some of the experiments gave lower results than those predicted from the intrinsic kinetics model. These represent the data with high catalyst loading or high conversion of hydrogen and nitroanisole. The deviations from the model predictions may be due to mass transfer limitations which were not considered in the intrinsic kinetics model. To confirm this observation, modeling of the microreactor was done under these reaction conditions with significant mass transfer effects. The modeling results were compared with the experimental data at different velocities and catalyst loading to determine the minimum gas–liquid mass transfer coefficient ($k_{gl}a_{gl}$). Then, the overall mass transfer coefficient (K_{la}) was calculated from the following equation:

$$\frac{1}{K_{la}} = \frac{1}{k_{gl}a_{gl}} + \frac{1}{k_{ls}a_{ls}} \quad (12)$$

Fig. 13 shows the overall mass transfer coefficient (K_{la}) values obtained by comparing these experimental results with the simulation results under different reaction conditions.

The figure clearly shows that the mass transfer coefficient is a function of overall linear velocity, and catalyst loading. The change in the mass transfer coefficient with the catalyst loading is because of the change in the overall flow velocity along the length of the reactor. As hydrogen is consumed along the length

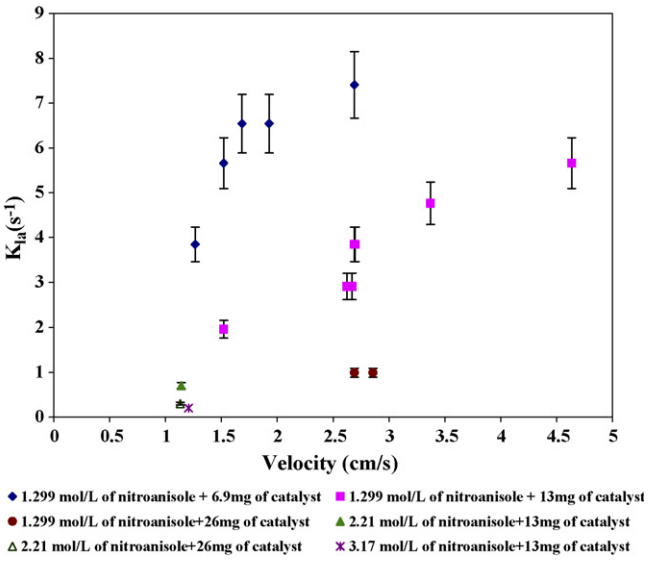

Fig. 13. Mass transfer coefficients in the microreactor as a function of overall velocity.

of the reactor, the length of the gas slug decreases resulting in a decrease in the overall flow velocity.

Fig. 13 shows that the mass transfer coefficients obtained in the packed-bed microreactor under the present experimental conditions range between 0.2 and $\sim 9\ s^{-1}$. These values compare favorably with the mass transfer coefficients obtained by Losey et al. [12] for the hydrogenation of cyclohexene in a packed-bed microreactor under similar reaction conditions. Hence, the range of mass transfer coefficient values obtained can be generalized to any hydrogenation reaction conducted in a packed-bed microreactor under these operating conditions. This range of mass transfer coefficients was used to determine the reaction times or residence times of the reactions that will be suitable for conducting kinetic study in the microreactor.

Assuming that any form of rate equation (Langmuir–Hinshelwood or power law) can be transformed into a pseudo-first order rate equation by combining all the terms in the rate expression except the concentration of limiting reactant into the rate constant. The rate expression will be of the form

$$r = k_r C_A \tag{13}$$

where r represents the rate of the reaction, k_r represents the intrinsic rate constant and C_A represents the concentration of the limiting reactant. The mass transfer coefficient values (K_{la}) must be much higher (at least 10 times) than intrinsic rate constants (k_r) for the reaction to be controlled by true intrinsic kinetics. From the range of mass transfer coefficients obtained, it indicates that the packed-bed microreactor can be used to obtain intrinsic kinetic information for hydrogenation reactions with intrinsic rate constants up to an order of magnitude of $10^0\ s^{-1}$, or with reaction half life times in the order of magnitude of 10^0 s and above.

3.3.2.3. Modeling of semi-batch reactor. The modeling for a semi-batch reactor was done similar to that of the microreactor. For the modeling of a semi-batch reactor, the contributions of various mass transfer resistances were assumed to be constant with time. The model used for the semi-batch reactor assumes the liquid to be ideally mixed, so that the composition of liquid is assumed to be uniform throughout the reactor. Considering the kinetics given by Eqs. (1) and (2), the rate of hydrogenation incorporating the effect of mass transfer will be given by the following equations.

3.3.2.4. Model for semi-batch reactor.

- Hydrogen concentration in bulk liquid

$$\frac{dC_{H,b}}{dt} = k_{ls}a_{ls}(C_{H,c} - C_{H,b}) + k_{gl}a_{gl}(C_{H,sat} - C_{H,b}) \tag{14}$$

- Hydrogen at catalyst

$$k_{ls}a_{ls}(C_{H,b} - C_{H,c}) = a_1(r_1 - r_2) \tag{15}$$

- *o*-Nitroanisole at the catalyst

$$\frac{dC_{nitro}}{dt} = a_1(-r_1) \tag{16}$$

In the above expressions, r_1 and r_2 are given by Eqs. (1) and (2), respectively.

Using Eqs. (14)–(16), the semi-batch reactor was modeled under different reaction conditions and the modeling results were compared with the experimental data obtained in the semi-batch reactor to evaluate the mass transfer coefficient. The liquid to solid mass transfer coefficient ($k_{ls}a_{ls}$) in the semi-batch reactor was calculated from the correlations in [3]. Fig. 14 shows the overall mass transfer coefficient (K_{la}) values estimated by comparing the conversion from the modeling results with the experimental data under different agitator speeds. The data clearly show that the mass transfer coefficient in the semi-batch reactor increases with increase in the stirrer speed. The mass transfer coefficient in the semi-batch reactor ranges from 0.01 to $0.07\ s^{-1}$. These are the typical values of mass transfer coefficients reported for batch [7] and other traditional laboratory reactors [19]. This implies that such reactors can be used to obtain intrinsic kinetic information for reactions with intrinsic rates constants (k_r) up to an order of

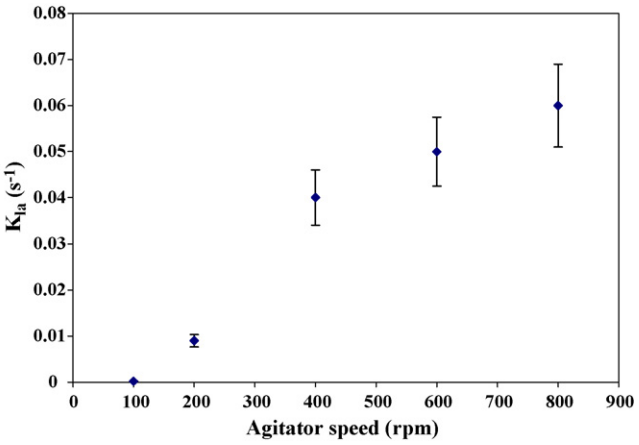

Fig. 14. Mass transfer coefficients in the semi-batch reactor as a function of stirrer speed.

magnitude of 10^{-2} s^{-1} or with half life times in the order of magnitude of 10^2 s and above. For the hydrogenation of *o*-nitroanisole, the half life time was calculated to be 4.8×10^2 s at a temperature of 30 °C, pressure of 100 psig, 1.299 mol/L *o*-nitroanisole concentration, and catalyst loading of 20 mg in a batch reactor. Hence, both batch and microreactors are suitable for conducting kinetic studies for this reaction.

In the above analysis, the conclusions on the reaction times suited for conducting kinetic studies in the batch and the microreactor are justified only for reactions which are first order with respect to hydrogen concentration. This analysis may be inaccurate for reactions with different reaction orders for hydrogen in which case the calculation becomes even more complicated.

From the above discussion, it can be clearly seen that the mass transfer coefficient values in the microreactor are two orders of magnitude higher than those of the semi-batch reactor. This is the result of much higher gas–liquid interfacial area in the microreactor than in the semi-batch reactor due to the turbulence created at the gas–liquid interface in liquid slugs. This tremendous increase in the mass transfer rate in the microreactor can be used not only to increase the productivity of extremely fast reactions but also to obtain intrinsic kinetic information for such reactions. The calculations showed that both batch and microreactors are suitable to obtain intrinsic kinetic information for hydrogenation reactions with half lives in the order of magnitude of 10^2 s and above, and microreactor is better suited to obtain intrinsic kinetic information for hydrogenation reactions with half lives in the order of magnitude between 10^0 and 10^2 s. If a batch reactor is used to obtain intrinsic kinetic study for these reactions, the reaction data would represent a mixture of intrinsic and mass transfer effects and hence would not provide information on true intrinsic kinetics. Therefore, a microreactor is more efficient than the conventional laboratory reactors in obtaining intrinsic kinetic data for fast hydrogenation reactions because of their high mass transfer and mixing characteristics.

4. Conclusions

Although several fast hydrogenation reactions have been conducted in microreactors, there are limited studies where a microreactor has been used for obtaining intrinsic kinetics for such fast reactions in spite of the excellent mass transfer it offers. Instead the kinetic study is conducted in conventional batch reactors. In the present study, the hydrogenation of *o*-nitroanisole was chosen as the model reaction to demonstrate that microreactor in addition to its other advantages over conventional reactors can be used as a tool to obtain intrinsic kinetic information. For this purpose, the performance of microreactor as well as that of a semi-batch reactor was evaluated. The kinetics of the hydrogenation of *o*-nitroanisole to *o*-anisidine was investigated in a semi-batch reactor using 2% Pd/zeolite catalyst. The reaction rates in the semi-batch reactor and the microreactor were found to be the same thereby confirming that the reaction is controlled by intrinsic kinetics in both reactors under similar conditions. Hence, the microreactor is as efficient as the semi-batch reactor in obtaining intrinsic kinetic data for this reaction.

The microreactor and the semi-batch reactor were modeled using the mass transfer model approach. The simulation results showed that the mass transfer coefficients in the microreactor are two orders of magnitudes higher than those of the semi-batch reactor. Further, the calculations showed that both batch and microreactors can be used for conducting kinetic studies for slow hydrogenation reactions with half lives in the order of magnitude of 10^2 s and above, and microreactor is better suited for conducting kinetic studies for hydrogenation reactions with half lives in the order of magnitude between 10^0 and 10^2 s.

Acknowledgements

This work is funded by the DOE-ITP under contract DE-FC36-03GO13156. The authors gratefully acknowledge the support. We would also like to acknowledge, our industrial partners from Bristol-Myers Squibb (BMS) especially Dr. Jale Muslehiddinoglu for her technical contributions to the study, Prof. Suphan Kovenklioglu for his helpful suggestions, and all the members of NJCMCS especially Dr. Raghunath Halder and Yuri Voloshin for their help throughout the research work.

References

[1] F. Roessler, Chimia 50 (1996) 106.
[2] M. Hoogenraad, J.B. Linden, A.A. Smith, Org. Process. Res. Dev. 8 (2004) 469.
[3] P.L. Mills, R.V. Chaudhari, Catal. Today 37 (1997) 367.
[4] K.R. Westerterp, H.J. Janssen, H.J. van der Kwast, Chem. Eng. Sci. 47 (1992) 4179.
[5] C.N. Satterfield, Mass Transfer in Heterogeneous Catalysis, M.I.T. Press, Cambridge, England, 1970, p. 86.
[6] K.B. Van gelder, J.K. Damhof, P.J. Kroijenga, K.R. Westerterp, Chem. Eng. Sci. 45 (1990) 3159.
[7] R.V. Chaudhari, M.G. Parande, P.A. Ramachandran, P.H. Brahme, Institute of Chemical Engineers Symposium Series No. 87, 1983, p. 205.
[8] E.J. Molga, K.R. Westerterp, Chem. Eng. Sci. 47 (1992) 1733.
[9] B.W. Hoffer, P.H.J. Schoenmakers, P.R.M. Mooijman, G.M. Hamminga, R.J. Berger, A.D. van Langeveld, J.A. Moulijn, Chem. Eng. Sci. 59 (2004) 259.
[10] J. Hajek, D.Yu. Murzin, Ind. Eng. Chem. Res. 43 (2004) 2030.
[11] M.T. Kreutzer, F. Kapteijn, J. Moulijn, Catal. Today 105 (2005) 421.
[12] M.W. Losey, M.A. Schmidt, K.F. Jensen, Ind. Eng. Chem. Res. 40 (2001) 2555.
[13] A. Gavriilidis, K.K. Yeong, R. Zapf, V. Hessel, Chem. Eng. Sci. 59 (2004) 3491.
[14] S. Tadepalli, R. Halder, A. Lawal, Chem. Eng. Sci. 62 (2007) 2663.
[15] P.H. Brahme, H.G. Vadgaonkar, P.S. Ozarde, M.G. Parande, J. Chem. Eng. Data 27 (1982) 461.
[16] D. Qian, A. Lawal, Chem. Eng. Sci. 61 (2006) 7609.
[17] T.A. Nijhuis, F.M. Dautzenberg, J.A. Moulijn, Chem. Eng. Sci. 58 (2003) 1113.
[18] M.T. Kreutzer, P. Du, J.J. Heiszwolf, F. Kapteijn, J.A. Moulijn, Chem. Eng. Sci. 56 (2001) 6015.
[19] M.H. Al-Dahhan, F. Larachi, M.P. Dudukovi, A. Laurent, Ind. Eng. Chem. Res. 36 (1997) 3292.